Supplementary Information

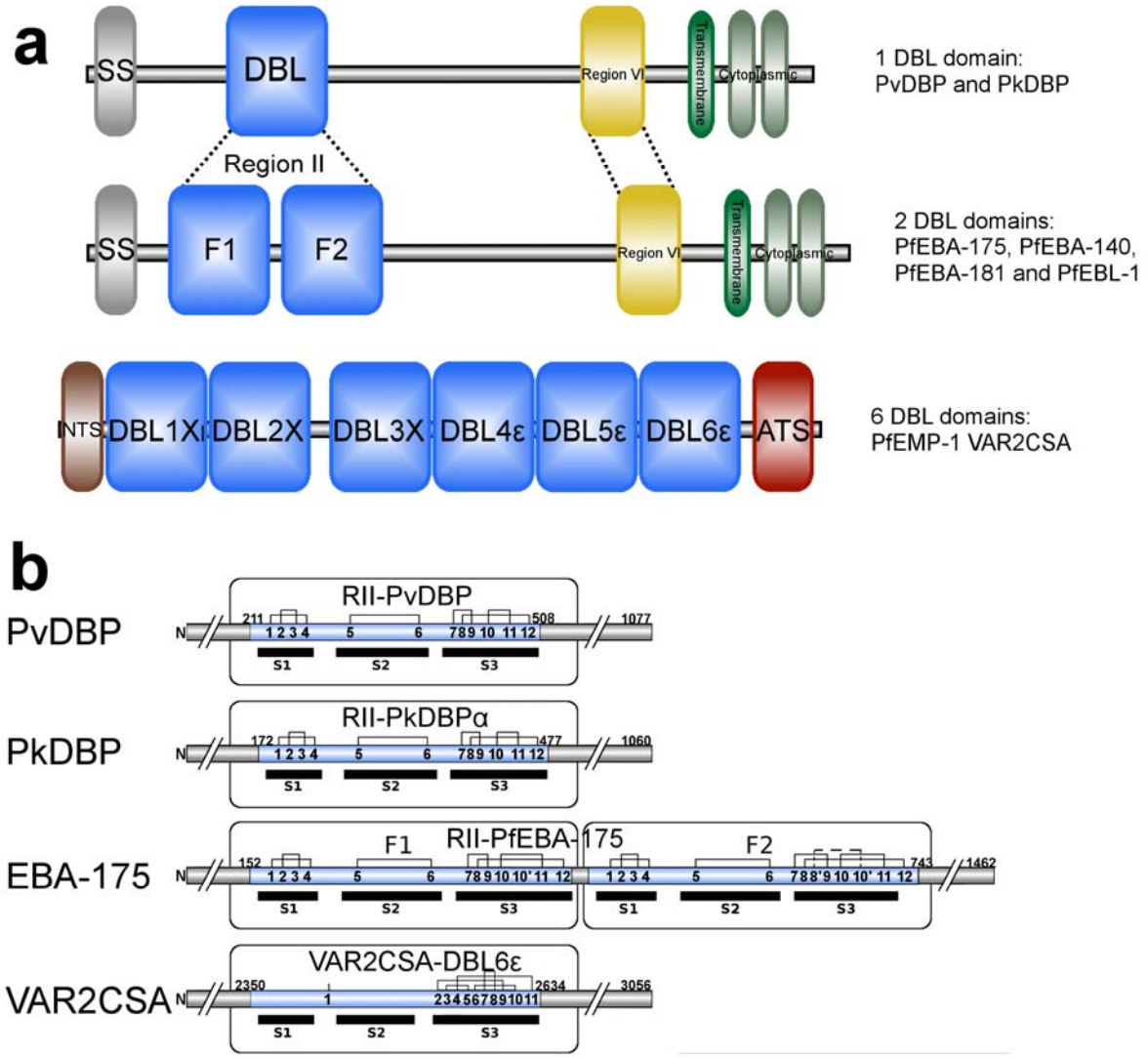

Supplementary Figure 1 DBL domain structures and disulfide bond patterns. (**a**) Top – domain structure of EBL proteins PvDBP and PkDBP. Middle – domain structure of EBL proteins PfEBA175, PfEBA-140, PfEBA-181 and PfEBL-1 with a duplication in Region II. Bottom domain structure of PfEMP1 VAR2CSA. Shown are the Signal Sequence (SS) in grey, region II or DBL domains in blue,

region VI in yellow, the transmembrane region in dark green, putative cytoplasmic domains in light green, the N-terminal sequence (NTS) in brown and the acidic terminal sequence (ATS) in red. (**b**) RII-PvDBP has a similar pattern of intra-subdomain disulfides as RII-PfEBA-175 (F1 and F2) and RII-PkDBP. RII-PfEBA-175 F2 has an additional disulfide bridge not found in other DBL domains (dashed line). VAR2CSA DBL6ε does not share this pattern of intra-subdomain disulfides. The DBL domains are colored light blue. Cysteines in the DBL domains are numbered and black lines represent disulfide linkages between cysteines. S1, S2 and S3 indicate subdomain 1, 2 and 3 respectively.

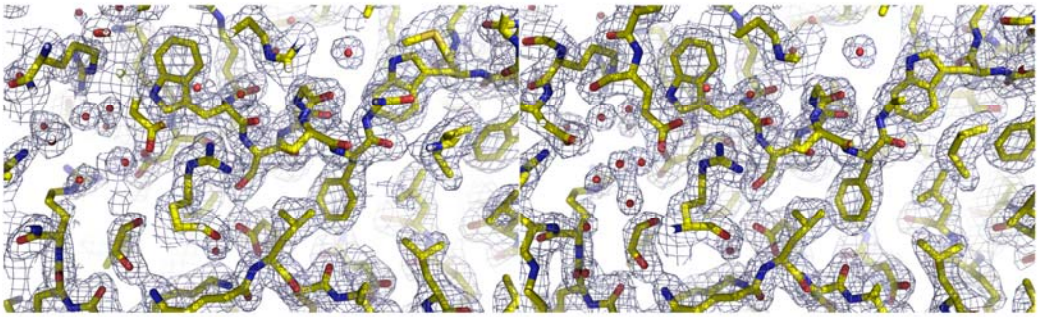

Supplementary Figure 2 Stereo view of the electron density map for a representative region of the RII-PvDBP structure**.**

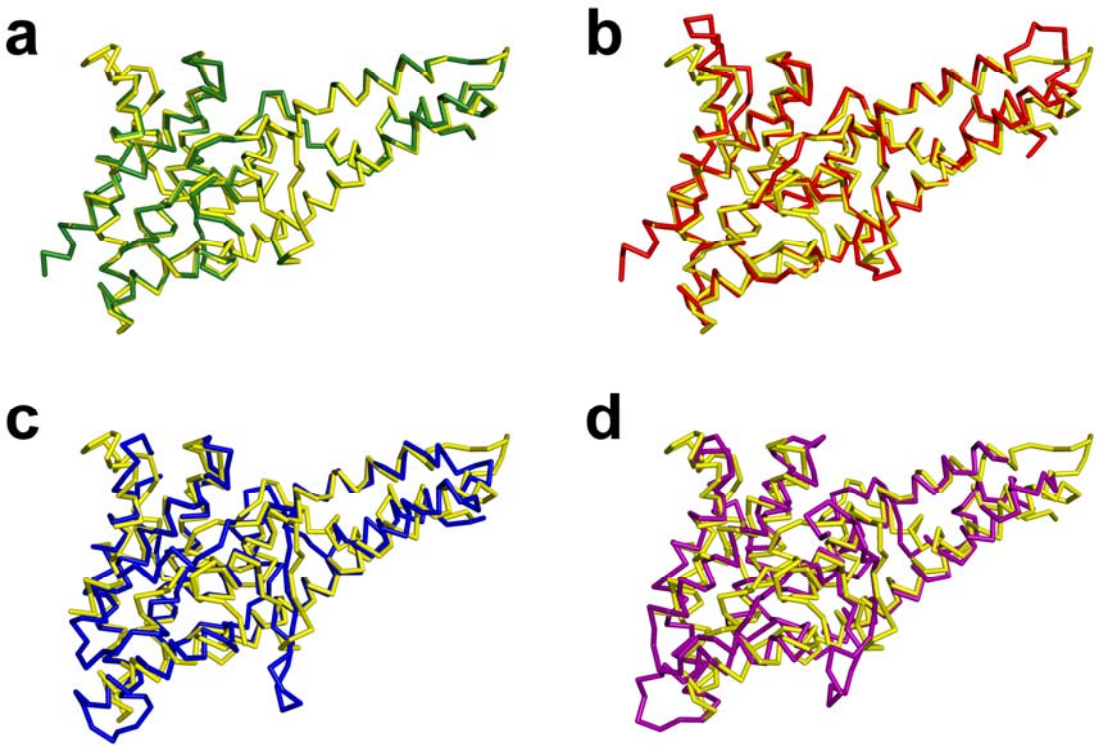

Supplementary Figure 3 RII-PvDBP has a similar DBL fold to RII-PfEBA-175 RII and RII-PkDBP**.** Structural alignments of: (**a**) RII-PvDBP chain B in yellow with RII-PvDBP chain A in green. (**b**) RII-PvDBP chain B in yellow with RII-PkDBP in red. (**c**) RII-PvDBP chain B in yellow with RII-PfEBA-175 F1 in blue. (**d**) RII-PvDBP chain B in yellow with PfEBA-175 F2 in purple.

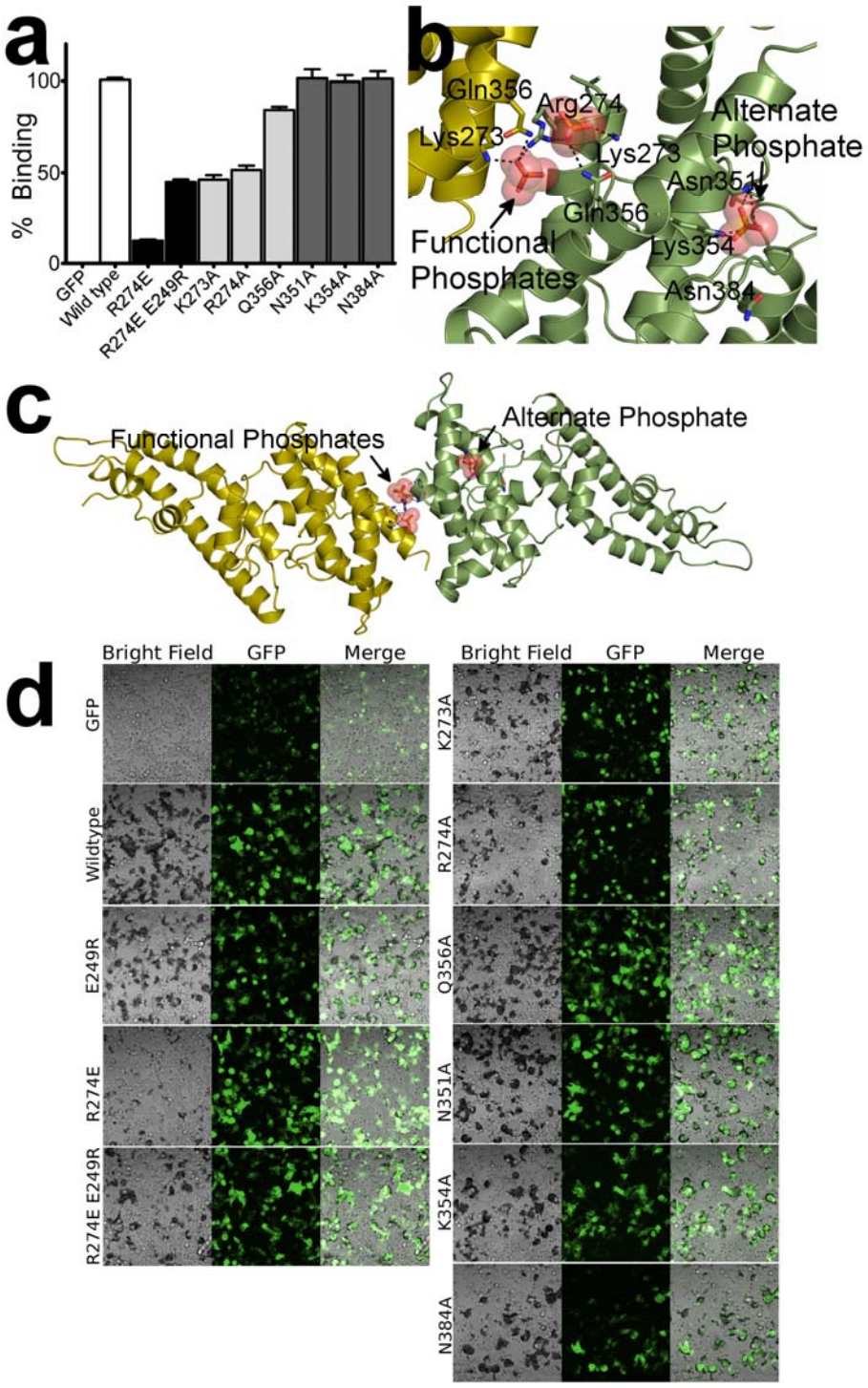

Supplementary Figure 4 Unlike the two phosphates at the RII-PvDBP dimer interface, mutation of residues coordinating an alternate phosphate has no

effect on RBC rosetting**.** (**a**) The percentage of HEK 293T cells expressing point mutants of GFP-RII-PvDBP which bind RBCs relative to wildtype, shown with standard error. White bar – wildtype. Black bars – dimer mutants and rescue. Light grey bars – sulfotyrosine binding mutants. Dark grey bars – alternate phosphate binding residues. (**b**) A detailed view of the functional phosphates and the alternate phosphate. (**c**) A global view of the functional phosphates and the alternate phosphate. (**d**) Bright-Field, GFP and merged confocal microscopic images of RBC rosetting experiments performed on HEK 293T cells expressing GFP, RII-PvDBP, RII-PvDBP E249R, RII-PvDBP R274E, RII-PvDBP R274E E249R, RII-PvDBP K273A, RII-PvDBP R274A, RII-PvDBP Q356A, RII-PvDBP N351A, RII-PvDBP K354A and RII-PvDBP N384A. Binding events are observed by clustering of dark smaller RBCs over the larger adherent HEK293T cells. Comparing bright field images of mutants to wildtype demonstrates deficiencies in binding.

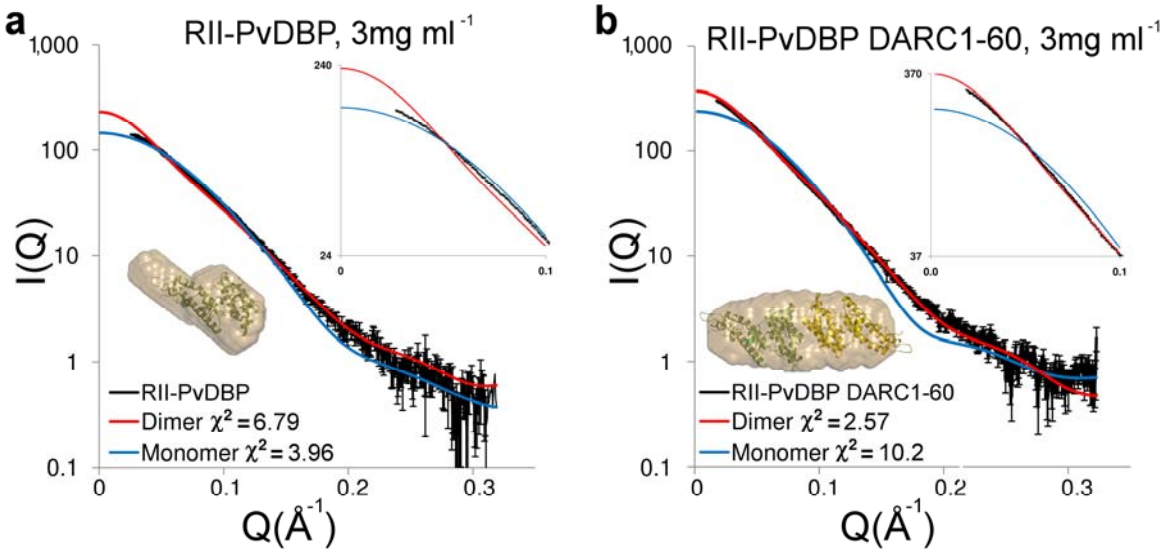

Supplementary Figure 5 SAXS data for RII-PvDBP and RII-PvDBP DARC1–60 at 3 mg ml^{-1}. Experimental (black) and theoretical SAXS plots for the monomer (blue) and dimer (red) at 3 mg ml^{-1}. An expanded plot of the low-angle data (0 < Q < 0.1) that clearly delineates oligomeric state is shown in the top right insert. *Ab initio* reconstructions are overlayed on structures (bottom left insert) with monomers colored in green and yellow and molecular envelopes in sand. (**a**) RII-PvDBP at 3 mg ml^{-1}. (**b**) RII-PvDBP DARC1–60 at 3 mg ml^{-1}.

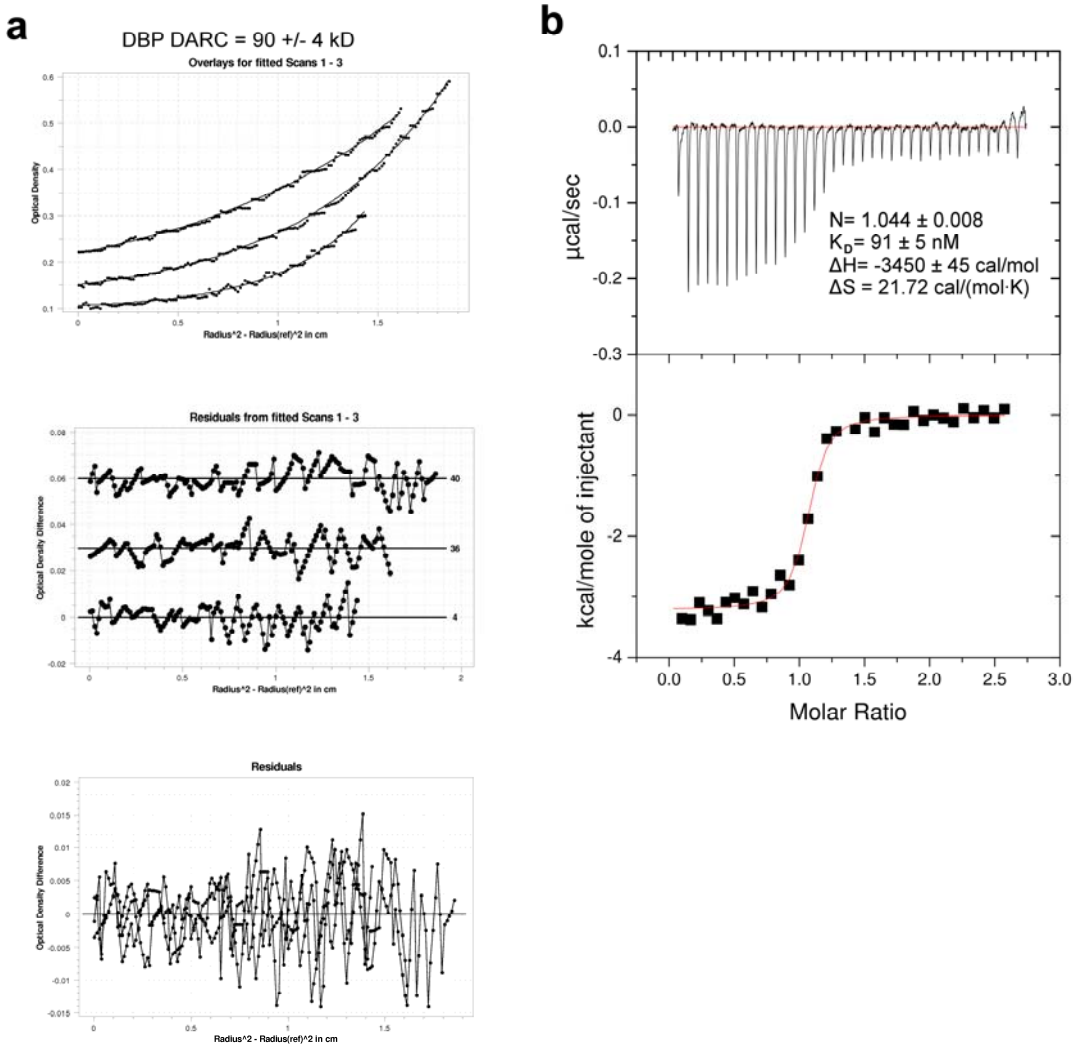

Supplementary Figure 6 AUC and ITC show DBP-DARC contains two molecules of RII-PvDBP bound to two molecules of DARC1–60. (**a**) AUC of RII-PvDBP DARC1–60 shows formation of a complex of two RII-PvDBP and two DARC1–60. Top panel - overlays of RII-PvDBP DARC1–60 at 3 mg ml^{-1}. Middle panel - individual residuals. Bottom panel - all residuals overlaid. (**b**) ITC of RII-PvDBP–DARC1–60 shows 1:1 stoichiometry of binding. Top – Raw ITC data of RII-PvDBP–DARC1–60. Bottom – Integrated ITC data.

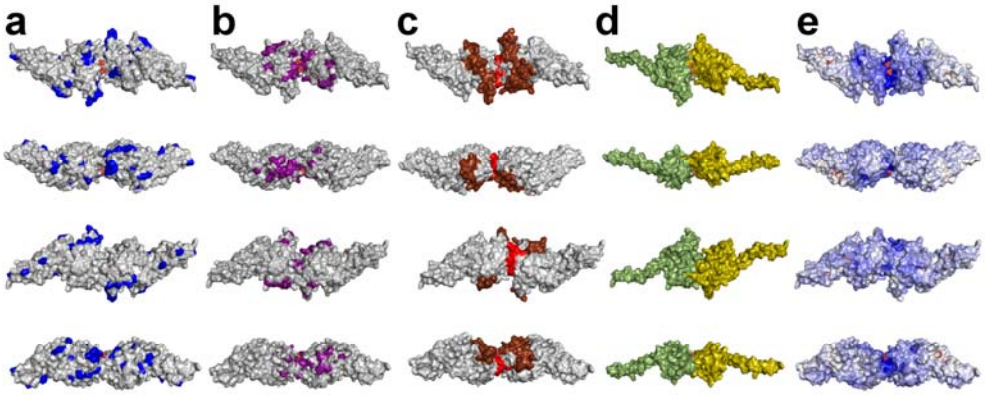
a
b
c
d
e

f

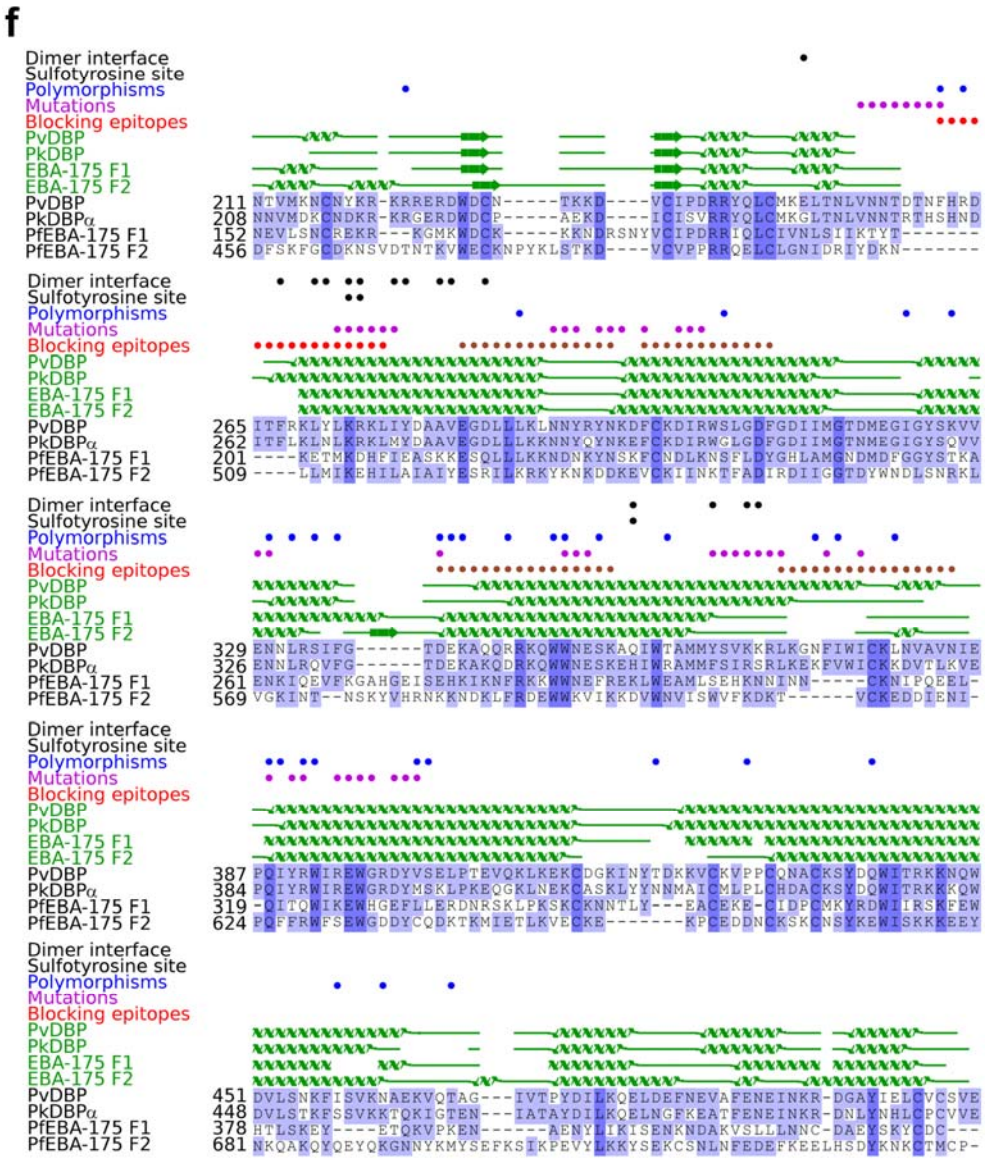
Dimer interface
Sulfotyrosine site
Polymorphisms
Mutations
Blocking epitopes
PvDBP
PkDBP
EBA-175 F1
EBA-175 F2
PvDBP 211 NTVMKNCNYKR-KRRERDWDCN-----TKKD-----VCIPDRRYQLCMKELTNLVNNTDTNFHRD
PkDBPα 208 NNVMDKCNDKR-KRGERDWDCP-----AEKD-----ICISVRRYQLCMKGLTNLVNNTRTHSHND
PfEBA-175 F1 152 NEVLSNCREKR---KGMKWDCK-----KKNDRSNYVCIPDRRIQLCIVNLSIIKTYT-------
PfEBA-175 F2 456 DFSKFGCDKNSVDTNTKVWECKNPYKLSTKD----VCVPPRRQELCLGNIDRIYDKN-------
Dimer interface
Sulfotyrosine site
Polymorphisms
Mutations
Blocking epitopes
PvDBP
PkDBP
EBA-175 F1
EBA-175 F2
PvDBP 265 ITFRKLYLKRKLIYDAAVEGDLLLKLNNYRYNKDFCKDIRWSLGDFGDIIMGTDMEGIGYSKVV
PkDBPα 262 ITFLKLNLKRKLMYDAAVEGDLLLKKNNYQYNKEFCKDIRWGLGDFGDIIMGTNMEGIGYSQVV
PfEBA-175 F1 201 ----KETMKDHFIEASKKESQLLLKKNDNKYNSKFCNDLKNSFLDYGHLAMGNDMDFGGYSTKA
PfEBA-175 F2 509 ----LLMIKEHILAIAIYESRILKRKYKNKDDKEVCKIINKTFADIRDIIGGTDYWNDLSNRKL
Dimer interface
Sulfotyrosine site
Polymorphisms
Mutations
Blocking epitopes
PvDBP
PkDBP
EBA-175 F1
EBA-175 F2
PvDBP 329 ENNLRSIFG------TDEKAQQRKQWWNESKAQIWTAMMYSVKKRLKGNFIWICKLNVAVNIE
PkDBPα 326 ENNLRQVFG------TDEKAKQDRKQWWNESKEHIWRAMMFSIRSRLKEKFVWICKKDVTLKVE
PfEBA-175 F1 261 ENKIQEVFKGAHGEISEHKIKNFRKKWWNEFREKLWEAMLSEHKNNINN-----CKNIPQEEL-
PfEBA-175 F2 569 VGKINT--NSKYVHRNKKNDKLFRDEWWKVIKKDVWNVISWVFKDKT------VCKEDDIENI-
Dimer interface
Sulfotyrosine site
Polymorphisms
Mutations
Blocking epitopes
PvDBP
PkDBP
EBA-175 F1
EBA-175 F2
PvDBP 387 PQIYRWIREWGRDYVSELPTEVQKLKEKCDGKINYTDKKVCKVPPCQNACKSYDQWITRKKNQW
PkDBPα 384 PQIYRWIREWGRDYMSKLPKEQGKLNEKCASKLYYNNMAICMLPLCHDACKSYDQWITRKKKQW
PfEBA-175 F1 319 -QITQWIKEWHGEFLLERDNRSKLPKSKCKNNTLY---EACEKE-CIDPCMKYRDWIIRSKFEW
PfEBA-175 F2 624 PQFFRWFSEWGDDYCQDKTKMIETLKVECKE-------KPCEDDNCKSKCNSYKEWISKKKEEY
Dimer interface
Sulfotyrosine site
Polymorphisms
Mutations
Blocking epitopes
PvDBP
PkDBP
EBA-175 F1
EBA-175 F2
PvDBP 451 DVLSNKFISVKNAEKVQTAG---IVTPYDILKQELDEFNEVAFENEINKR-DGAYIELCVCSVE
PkDBPα 448 DVLSTKFSSVKKTQKIGTEN---IATAYDILKQELNGFKEATFENEINKR-DNLYNHLCPCVVE
PfEBA-175 F1 378 HTLSKEY----ETQKVPKEN-------AENYLIKISENKNDAKVSLLLNNC-DAEYSKYCDC---
PfEBA-175 F2 681 NKQAKQYQEYQKGNNYKMYSEFKSIKPEVYLKKYSEKCSNLNFEDEFKEELHSDYKNKCTMCP-

Supplementary Figure 7 Additional views of Figure 4, rotated by 90 ° along the x-axis and sequence and structural similarity between DBL domains. (**a**) Polymorphic residues of RII-PvDBP (blue) mapped onto the RII-PvDBP dimer. (**b**) Alanine substitutions which abrogate RII-PvDBP-RBC rosetting (purple). (**c**) Epitopes recognized by blocking antibodies (red – most significant, brown – significant). (**d**) The minimal binding domain of RII-PvDBP. (**e**) Electrostatic mapping of the RII-PvDBP dimer. (**f**) Sequence and structural similarity between DBL domains of PvDBP, PkDBP, and PfEBA-175 F1 and F2. Secondary structure is shown in green. Circles above the alignment indicate important residues (polymorphisms - blue, mutations - purple, blocking-antibody epitopes – red and brown, dimer interface or sulfotyrosine site - black). Dark and light blue shading indicates invariant and conserved residues respectively. Accession numbers for sequences are XP_001608387, XP_002261904 and XP_001349207 for PvDBP, PkDBP alpha and PfEBA-175 respectively.

Supplementary Methods

Isothermal Titration Calorimetry. RII-PvDBP and DARC1–60 were dialyzed overnight against buffer containing 50 mm sodium chloride and 20 mM 4-(2-hydroxyethyl)-1-piperazineethanesulfonic acid (HEPES) pH 7.4. ITC experiments were carried out at 10 °C using a VP-ITC instrument (MicroCal). The cell contained 1.4 ml of 20 μm RII-PvDBP, and DARC1–60, at a concentration of 200 μm, was titrated in 37 injections of 8 μl each. Traces were corrected by subtracting blank measurements of DARC1–60 injected into the ITC buffer and analyzed using Origin Version 5.0 (MicroCal). Stoichiometry and binding constants were calculated by fitting the integrated data to a one-site binding model. Protein concentrations were determined by absorbance measurements under denaturing conditions (6 M guanidinium hydrochloride, 10 mM dithiothreitol).

Analytical Ultracentrifugation. DARC1–60 was labelled with Cy3 N-hydroxysuccinimide (NHS) ester. Cy3-NHS ester (Lumiprobe) was incubated with DARC1–60 for two hours at room temperature in 0.1 M sodium bicarbonate pH 8.5 with a 10-fold molar excess of Cy3-NHS ester. DARC1–60 was then purified from excess Cy3-NHS ester by size exclusion chromatography. DARC1–60 has no lysines and is therefore singly labelled by Cy3 at the N-terminus.

Sedimentation equilibrium experiments were performed using a Beckman model XL-A analytical ultracentrifuge. RII-PvDBP and DARC1–60 were first purified separately using size exclusion chromatography into 50 mm sodium

chloride and 20 mM HEPES pH 7.4 to remove any trace amounts of aggregate. RII-PvDBP and DARC1–60 were mixed in an equimolar ratio. Data were acquired using six-hole cells at an average of three absorbance measurements at 575 nm, with a radial spacing of 0.002 cm and at a temperature of 10 °C. Data, collected at 9k, 12k and 15k RPM at 3 mg ml^{-1} of RII-PvDBP–DARC1–60 were analyzed using a single component model using UltraScan Analysis 9.4.